

Premartensitic phenomena in the ferro- and paramagnetic phases of Ni₂MnGa

U. Stuhr

Paul Scherrer Institut, 5232 Villigen, Switzerland

P. Vorderwisch

Hahn-Meitner-Institut, 14109 Berlin, Germany

V. V. Kokorin

Institute of Magnetism, 252680 Kiev, Ukraine

P.-A. Lindgård

Risø National Laboratory, 4000 Roskilde, Denmark

(Received 6 August 1997)

Low-energy phonons were studied in the ferromagnetic and paramagnetic phases of the Heusler alloy Ni₂MnGa. The investigated sample shows a martensitic phase transformation with a transition temperature $T_M \approx 284$ K, only about 80 K below the Curie temperature. Therefore, premartensitic phenomena could be studied in the ferromagnetic as well as in the paramagnetic state. The $(\xi \xi 0)$ TA₂-phonon branch shows a strong but incomplete softening at $\xi \approx 1/3$ in the premartensitic phase when the temperature approaches T_M . The temperature dependence of this softening changes at the Curie temperature which can be explained by an additional contribution of the magnetization to the Landau free energy. At the wave vector of the strongest phonon softening a central peak occurs. A second elastic peak, with the same temperature behavior, appears at $\xi \approx 0.17$. The relation of these elastic precursors to the low-temperature structure is discussed. [S0163-1829(97)02846-4]

I. INTRODUCTION

Metallic systems which undergo martensitic transformations on cooling exhibit diverse phenomena as they approach their transformation temperature. In spite of their frequent occurrence, the understanding of these phenomena and of the transformation process itself is quite incomplete.¹ Martensitic transformations, characterized as shear dominant, lattice-distortive, diffusionless transformations occurring by nucleation and growth,² are necessarily of first order. Based on the strength of the discontinuous character of the transition, different groups of metallic systems have been classified, ranging from strongly first-order, through moderately or weakly first-order, to nearly second-order transforming materials.³ Whereas the first group does not show any (significant) evidence of instabilities of the parent phase, the last two groups reveal a variety of *precursor* (or *pretransitional*) phenomena when the martensitic transition temperature is approached. As a martensitic transformation may occur without any lattice-dynamical signature, precursor effects are therefore not a universal feature, but illuminate the underlying physics of the transformation.⁴

Precursor phenomena can be observed as anomalies in phonon dispersion curves: anomalously low-energy phonon branches with correspondingly small elastic stiffness constants and, if shuffles are involved, the occurrence of strong phonon anomalies (*soft phonons*) for wave vectors $\mathbf{q} \neq 0$ and elastic intensity (*central peaks*) at the same wave vectors. The terms in brackets, usually known in context with second-order transitions, have been reinterpreted in a phenomenological Landau theory for first-order transitions.^{5,6}

Experimentally, inelastic and elastic neutron scattering has been applied to study dynamical and static phenomena in the parent phase near the transformation. A very recent study⁷ of Co, an example for a strong first-order transformation, showed neither dynamical nor static anomalies, with the conclusion that the martensitic phase transformation is less affected by phonon anomalies and that excess entropy caused by low-energy modes in the parent phase is less important. The extensively studied shape-memory alloy Ni_xAl_{1-x} (Refs. 8 and 9) is a prototypical example for a moderate first-order transition which, for $x=0.625$, is from a bcc ($B2$) structure to a modulated $7R$ product phase. Pronounced phonon anomalies (an unusually low-energy TA₂ phonon branch and an anomalous temperature-dependent, incomplete phonon softening at a particular wave vector $\mathbf{q} \neq 0$ of this branch) and diffuse elastic scattering (central peak) occurring at the same wave vector \mathbf{q} have been observed. These anomalies are directly related to the evolution of premartensitic structural configurations, which are viewed as embryos of the product martensite.¹⁰

The model system Ni₂MnGa investigated in this paper is the only ferromagnetic Heusler alloy known to undergo a martensitic transformation upon cooling. The martensitic transformation is from a cubic ($L2_1$) high-temperature phase to a modulated tetragonal martensitic phase.¹¹ Further intermartensitic transformations can be induced by stress.¹² Depending on the atomic ordering, the Curie temperature T_C ranges from 360 to 395 K, whereas the martensitic transformation start temperature T_M is extremely sensitive to composition. Values between 175 and 450 K are reported in the literature. The transformation is thermoelastic, and the shape memory behavior of Ni₂MnGa has been confirmed.¹³ Within

the classification cited above,³ the system should be member of the group with a moderate or weak first-order transition.

A recent neutron-scattering investigation of Ni₂MnGa on a single crystal with $T_M \approx 220$ K (Ref. 14) showed indeed a strong, though incomplete, softening in the $[\xi \xi 0]$ TA₂-phonon branch at a wave vector $\xi_0 \approx 0.33$ and, for the same wave vector, elastic diffuse scattering. This wave vector is completely different from that expected for a five-layer ($\xi_M = 0.4$) modulation of the martensitic phase.¹²

We present inelastic and elastic neutron-scattering data taken on a sample with $T_M \approx 284$ K. This temperature is about 65 K higher and closer to T_C (≈ 364 K for our sample) than the value of T_M used in the previous study.¹⁴ This allows us to investigate precursor phenomena not only in the ferromagnetic, but also in the paramagnetic state. It is the aim of this paper to discuss a significant effect on the phonon softening, observed when passing the magnetic transition at T_C , and to relate further observed precursor effects to the underlying transformation process.

II. SAMPLE AND EXPERIMENT

The Ni₂MnGa single crystal (size about $20 \times 10 \times 10$ mm³) was grown without a seed crystal in a high-frequency induction furnace under an argon atmosphere by the Bridgman method. The actual chemical composition was 51.5 at. % Ni, 23.6 at. % Mn, and 24.9 at. % Ga. Susceptibility measurements, performed with a superconducting quantum interference device (SQUID) magnetometer, yielded a Curie temperature of (364 ± 1) K.

The martensitic phase transition temperature T_M could be determined from the temperature dependence of the (2 2 0) reflection of the cubic lattice, which disappears in the low-temperature phase, as well as with susceptibility measurements to (284 ± 1) K. The transition temperature of the reverse process was about 6 K higher. The single-crystal high-temperature phase could be recovered, with only a slight increase in mosaic spread, in this reverse process.

The neutron-scattering experiments were performed at the HMI reactor at the triple-axis spectrometer for cold neutrons V2 (FLEX). The sample was mounted in a cryofurnace (temperature accuracy ~ 1 K) with the [001] crystal axis perpen-

dicular to the scattering plane. The neutron spectra were taken with fixed final neutron wave vectors k_f [preferentially 1.2 and 1.8 Å⁻¹ in the (2 0 0) and the (2 2 0) Brillouin zone, respectively]. To avoid contamination of higher-order neutrons, a cooled Be filter was inserted in the primary beam when a final wave vector $k_f = 1.2$ Å⁻¹ was used. No filter was necessary for $k_f = 1.8$ Å⁻¹, since the higher-order neutrons are suppressed by the curved neutron guide. Nevertheless, for some of the elastic measurements a check with a tunable PG filter¹⁵ was made in order to prove that the small amount of second-order neutrons has no influence on the spectra. The elastic energy resolutions [full width at half maximum (FWHM)] were 35 and 150 μeV for $k_f = 1.2$ and 1.8 Å⁻¹, respectively.

III. RESULTS AND DISCUSSION

A. Phonon dispersion

In Fig. 1 the low-energy part of the $[\xi 0 0]$ and $[\xi \xi 0]$ phonon branches are shown. All phonons with $(\xi 0 0)$ propagation and the $(\xi \xi 0)$ -TA₂ phonons with $\xi \leq 0.04$ have been measured in the (2 0 0) Brillouin zone, the others in the (2 2 0) zone. The dashed lines indicate extrapolations of the sound velocity results of Refs. 16 and 17. The initial slopes of the phonon dispersion curves at small reduced wave vectors ξ are, with the exception of the transverse TA₂ phonons ($[\xi \xi 0]$ propagation direction and $[1 - 1 0]$ polarization), in good agreement with these ultrasonic measurements. The slope of the TA₂-phonon dispersion curve has, even for the lowest investigated ξ values ($\xi = 0.02$), only about one-third of the value than expected from these sound velocity results. Very recent published data of ultrasonic experiments,¹⁸ however, are in good agreement with the presented results. They are indicated in Fig. 1 as a dotted line.

B. Soft phonon

The most characteristic feature of the phonon dispersion curves of Ni₂MnGa is the softening of the TA₂ mode when the temperature approaches the martensitic phase transition temperature. The strongest softening occurs for ξ values of about 0.33. This result is in accordance with previous results of x-ray- and neutron-scattering measurements.^{14,19} Some phonon spectra of this mode at various temperatures are shown in Fig. 2. The excitation energy decreases on cooling, while the phonon intensity increases, as expected for a soft-mode behavior. However, the phonon energy does not approach zero at the phase transition temperature. Even the spectrum measured at 284.6 K less than 1 K above the phase transition temperature, shows a pronounced phonon peak with a maximum at approximately 0.9 meV. Although the peak width has increased compared to those measured at higher temperatures, which might be caused by internal stresses, the phonon is not overdamped. The other spectra of Fig. 2 show only a small temperature dependence of the linewidth, but all widths are much larger than the instrumental resolution of 0.15 meV, indicating a strong phonon damping. The lower intensity of the phonon at 284.6 K compared to the spectra measured at higher temperatures can be explained by a partial transformation of the sample into the tetragonal low-temperature phase. This was proved by the

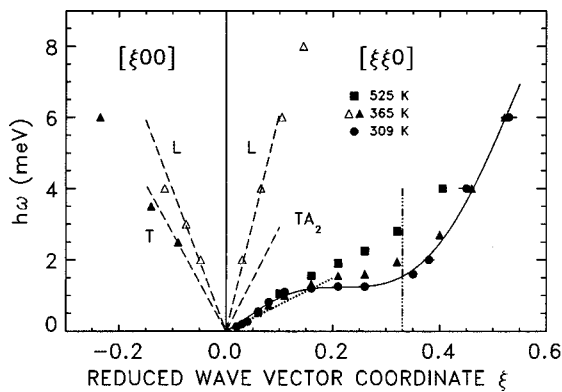


FIG. 1. Low-energy part of the $(\xi \xi 0)$ and $(\xi 0 0)$ phonon branches. The open symbols represent the longitudinal phonons, the solid ones transverse phonons. The dashed lines are extrapolations of sound velocity results from Refs. 16 and 17, the dotted line that from Ref. 18 for the TA₂ mode.

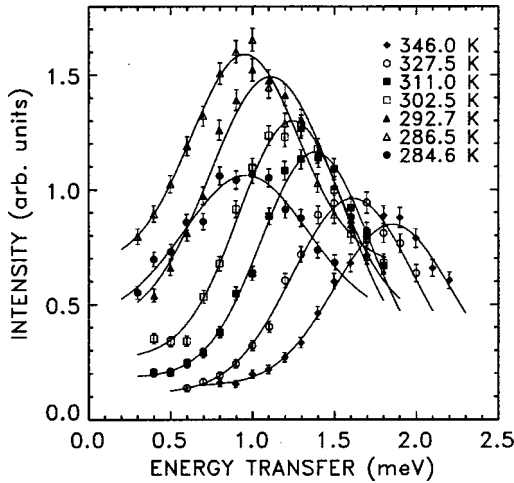


FIG. 2. Spectra of the TA_2 soft phonon at $\xi=0.33$ for different temperatures. Note that the intensity of the phonon at the lowest temperature ($T=284.6$ K) is lower because a part of the sample is already in the tetragonal phase. The lines are guides to the eye.

comparison of the intensities of the $(2\ 2\ 0)$ Bragg peak of the cubic phase which showed a comparable decrease in intensity. The incomplete softening TA_2 mode for $\xi=0.33$ was also observed for the sample investigated in a previous study,¹⁴ but in contrast to the present study, that sample showed an increase of the phonon energy close to the phase transition temperature. Such an increase of the phonon energy is an indication for an intermediate phase. We could not find any indication of such a phase, neither in the phonon behavior nor in elastic measurements. Therefore, we can exclude an intermediate phase at least at temperatures more than 2 K above T_M . There are further distinctive differences compared to the previous results.¹⁴ The width in ξ where softening occurs is much broader than reported in the previous study, indicating a shorter coherency length of the phonon (we remark that the resolution in ξ is comparable in both measurements). One consequence from this is that the dispersion curve of our sample shows only a very weak minimum.

In Fig. 3 the square of the soft phonon energy, measured

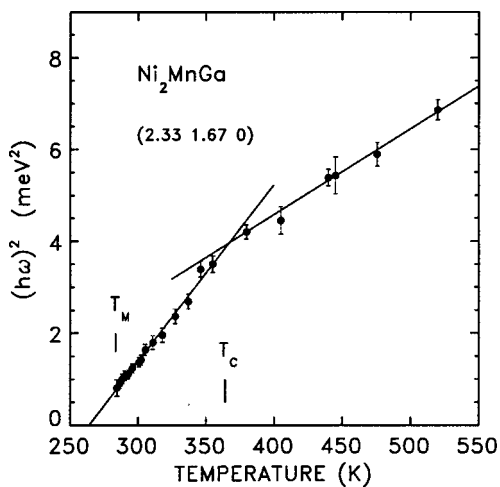


FIG. 3. Plot of the squared energy of the soft phonon vs the temperature. The lines are guides to the eye.

at $\xi=0.33$, is plotted versus the temperature. The figure shows again that there is a finite phonon energy at the phase transition temperature. Starting from this value, the square of the phonon energy increases linearly, as expected from soft-mode theory,²⁰ up to the Curie temperature. Above the Curie temperature there is also a linear dependence, but there is a distinct change of the slope a from 0.039 $(\text{meV})^2/\text{K}$ below T_C to 0.019 $(\text{meV})^2/\text{K}$ above T_C . The extrapolated temperatures for the dynamical lattice instability T_1 are 264 and 175 K for the ferro- and paramagnetic states, respectively. This indicates that the phonon softening depends on the magnetic ordering in the sample. The slope a in the ferromagnetic phase is slightly lower than of the a sample with $T_M \approx 220$ K.¹⁴

The incomplete softening of the phonon could be expected, since the martensitic phase transition in Ni_2MnGa is a first-order transition. The conventional Landau theory, predicting a complete phonon softening, applies only for second-order transitions. In this theory the free energy F of the system is given by

$$F = A\eta^2 + C\eta^4 + \dots, \quad (1)$$

where C is approximately constant. The temperature dependence of the system is mainly through the parameter A which can be expanded near T_M as $A' (T - T_M)$ with constant A' . η is the order parameter, which, in case of soft mode systems, is the lattice distortion caused by the soft phonon. Two extensions of this ansatz have been proposed to describe first-order phase transitions: (i) the use of an asymmetric potential by introducing a cubic term of the order parameter,^{21,6} which, however, is not applicable for the present system because of symmetry reasons (see Sec. III C), and (ii) to introduce a term with the sixth power of the order parameter and a negative C .^{21,22} A negative temperature-dependent C can be understood in terms of a coupling between a uniform and $\mathbf{q} \neq 0$ modulation, needed for the martensitic transformation.⁵ The free energy can thus be written as

$$F = A\eta^2 + C\eta^4 + D\eta^6. \quad (2)$$

In this case a first-order phase transition occurs if the condition $AD/C^2 = 1/4$ is fulfilled. Again, we will use the assumption that in a certain temperature range the temperature dependence of A can be well approximated by $A = A'(T - T_1)$. A consequence of this description is that the energy of the soft phonon, $\hbar\omega_p$, above the phase transition temperature is

$$(\hbar\omega_p)^2 = a(T - T_1), \quad (3)$$

where a is a constant. At $T = T_1$ the lattice would become dynamically unstable; however, the phase transition occurs already at a higher temperature $T_M = T_1 + C^2/(4A'D)$. Conclusively, the softening of the phonon cannot be complete. Since the assumption of the temperature dependence of A (and the negligible temperature dependence of C and D) is only justified in a limited temperature range near the phase transition temperature (or more precisely near T_1), Eq. (3) might only hold in a limited temperature range. Nevertheless, the kink in the temperature dependence of the phonon energy must be related to the magnetic ordering, since such a

deviation from Eq. (3) has neither been found for the sample with $T_M=220$ K, measured only within the ferromagnetic phase,¹⁴ nor, to our knowledge, in any other system. If the validity range of Eq. (3) is extended, we would expect a smooth deviation from a linear deviation and finally approaching a nearly-temperature-independent phonon energy, whereas we observe an approximately constant slope in the paramagnetic state.

The coincidence of the Curie temperature and the temperature where the kink occurs suggests that the magnetization of the sample influences the phonon energy. This can be described in Eq. (2) by introducing an additional term to the free energy of the system which contains a function of the magnetization. The occurrence of such a term can be expected if magnetoelastic effects are considered.

However, the kink in Fig. 3 can be principally explained by two different effects of the magnetization, either by interaction with the macroscopic magnetization—this would mainly influence the phonon in the ferromagnetic phase—or, at least in principle, by an interaction with the short-range magnetic fluctuations. The first interaction has its major temperature dependence in the ferromagnetic phase, the latter one in the paramagnetic phase. In the first case the interaction between the magnetization and the soft phonon potential would be indirect, since the magnetization would influence the elastic moduli which then causes a change in the soft phonon behavior. An indication for this interpretation might be the strong temperature dependence of the sound velocity between T_M and T_C .^{16,17} Unfortunately, there are no experimental data for temperatures above T_C , which could prove this interpretation. Furthermore, since we can expect an interaction potential proportional to the square of the magnetization M with $M \sim (1 - T/T_C)^{1/2}$, such an interaction would change the slope a , but not the linear behavior, in agreement with our observation. This interaction between the magnetization and phonons has been observed for the Invar alloys Fe_3Pt and $\text{Fe}_{1-x}\text{Pd}_x$, which show a soft mode at the Γ point.^{23,24}

The second case would be a direct interaction between the magnetic fluctuations and the soft phonon potential. In a previous study²⁵ magnons were observed up to 520 K, showing that magnetic fluctuations on the length scale probed by neutron scattering still exist at these temperatures.

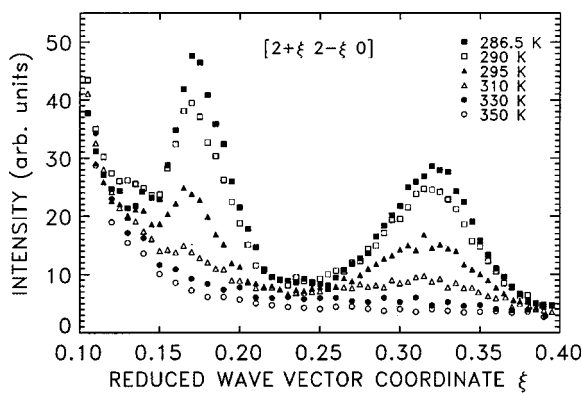


FIG. 4. Elastic scattering at $\mathbf{q}=(2+\xi 2-\xi 0)$ at various temperatures.

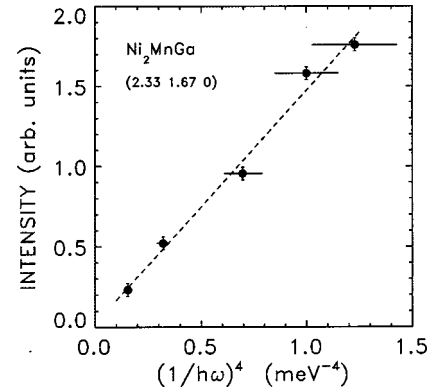


FIG. 5. Plot of the central peak intensity vs the fourth power of the reciprocal value of the soft phonon energy. The values of soft phonon energy were taken from the interpolation line in Fig. 3, with error bars corresponding to those of the experimental values.

C. Elastic scattering

The elastic scattering in the $(2\ 2\ 0)$ Brillouin zone in the transverse $[\xi - \xi\ 0]$ direction is shown in Fig. 4 for different temperatures. With decreasing temperature a strong central peak appears at $\xi=0.33$. Since the softening of the phonon occurs in a quite broad ξ region, the central peak shows more clearly that the origin of the phonon instability is at $\xi \cong 0.33$. This value is surprising since, for the structure of the low-temperature phase, a five- (or seven-) layer modulation was reported.^{12,26} Such a modulation period in the cubic phase would cause a central peak at $\xi=0.4$ (or $\xi=0.28$). A second elastic peak occurs at $\xi=0.17$ with about the same temperature dependence as the central peak at $\xi \cong 0.33$. This peak was also observed in an x-ray study¹⁹ and was attributed to a splitting of the $(2\ 2\ 0)$ Bragg peak. Both peaks show no quasielastic broadening, and their widths in longitudinal direction are only resolution limited ($\Delta\xi \approx 0.01$).

In Fig. 5 the central peak intensity I_{CP} is plotted versus the fourth power of the reciprocal value of the soft-mode energy. The straight line demonstrates that the data can be described by $I_{CP} \sim (\hbar\omega)^{-4}$. This is the expected relation between a soft mode and its induced central peak.^{27,28} Figure 6 shows a spectrum taken at $\xi=0.33$ in an energy range which includes the central peak and the soft phonon in up and down

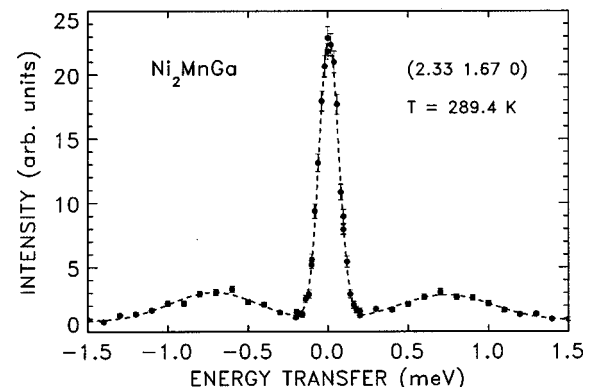


FIG. 6. Example spectrum of the soft phonons and the central peak at $\mathbf{q}=(2.33\ 1.67\ 0)$ and $T=289.4$ K. The peak height of the incoherent elastic contribution is about 3.

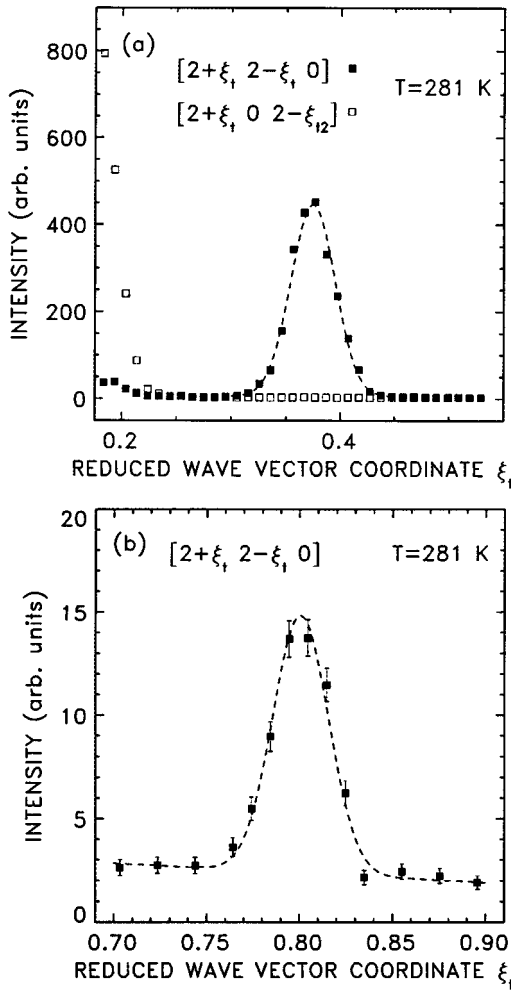


FIG. 7. (a) and (b) show elastic scans in the martensitic phase at $T=281$ K at different ξ ranges. The solid squares represent the intensities of scans along $(2 + \xi_t, 2 - \xi_t, 0)$, the open symbols scans along $(2 + \xi_t, 0, 2 - \xi_{t2})$. The errors in (a) are smaller than the data points.

scattering. The spectrum shows the broadened peaks of the damped phonon in comparison with the resolution-limited linewidth of the central peak.

For a better understanding of the elastic peaks, a comparison with the structure of the low-temperature phase is helpful. In an ideal case, the $(2\ 2\ 0)_{\text{cubic}}$ reflection would split in the low-temperature phase into one $(2\ 2\ 0)_{\text{tet}}$ and one $(2\ 0\ 2)_{\text{tet}}$ reflection. However, since the single crystal of the high-temperature phase decomposes in the low-temperature phase into several variants with somewhat different orientations, we can expect several Bragg reflections. Fortunately, it turned out that there were only two $(2\ 2\ 0)_{\text{tet}}$ and one $(2\ 0\ 2)_{\text{tet}}$ strong Bragg reflections and a few reflections with much lower intensities. The tetragonal distortion described by the ratio of the lattice constants calculated from the two reflections is $c/a=0.94$, in agreement with previous results.^{11,12} The orientations of the two crystallites with (220) reflections in the scattering plane differ by about 2.1° , which allows an unambiguous assignment of elastic peaks in transverse scans to one of the crystallites at least for $\xi_t \geq 0.2$. ξ_t and ξ_{t2} indicate the reduced wave vectors of the tetragonal phase in $[1\ 0\ 0]$ and $[0\ 0\ 1]$ directions, respectively.

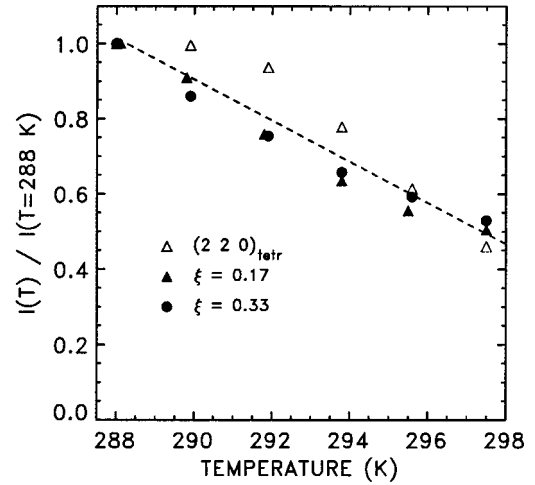


FIG. 8. Temperature dependence of the integral intensities of the precursors in the cubic phase, normalized to their intensity at 288 K. The open data points are the precursors of the tetragonal $(2\ 2\ 0)$ Bragg peak, the solid data points the precursors at $(2 + \xi_t, 2 - \xi_t, 0)$ with $\xi_t=0.17$ (triangles) and $\xi_t=0.33$ (circles).

Figures 7(a) and 7(b) show such elastic transverse scans in the tetragonal phase. The origins of the scales are the positions of the strongest reflection of each kind. The transverse scan from the $(2\ 0\ 2)$ reflection shows a broad region with a very high intensity up to $\xi_t \approx 0.2$, a consequence of the high mosaicity in the low-temperature phase and no significant structure at higher wave vectors. On the other hand, the spectrum with origin in the $(2\ 2\ 0)$ reflection shows reasonable small Bragg reflections and an additional peak at $\xi_t = 0.38$. This second peak can be attributed to the five-layer modulation found in previous studies.^{12,26} This interpretation is supported by the appearance of a harmonic of the modulation which is shown in an extension of the spectrum to higher ξ_t values in Fig. 7(b). The harmonic peak has approximately 5% of the intensity of the peak at $\xi_t = 0.38$. Thus the modulation occurs only in the $[\xi_t, \xi_t, 0]$ direction of the tetragonal phase, perpendicular to the tetragonal distortion, and the symmetry of the soft phonon potential will not be disturbed by tetragonal precursors which justify the rejection of a cubic term in the free energy in Sec. III B. Both spectra were taken with a tunable PG filter in order to reduce the second-order neutrons as well as possible (but no significant differences have been found to spectra taken without this filter).

Since the origin of the $(2\ 2\ 0)_{\text{tet}}$ reflection is shifted by $\Delta \xi_t \sim 0.046$, the position of the superstructure peak is in the coordinate system of the cubic phase at the position of the central peak at $\xi_t = 0.33$. Consequently, the central peak is a precursor of the five-layer modulation of the tetragonal phase. There are also precursors of the tetragonal Bragg peaks in the cubic phase. The temperature dependence of the intensities of the tetragonal Bragg peaks, the central peak at $\xi_t = 0.33$, and the peak at $\xi_t = 0.17$ are compiled in Fig. 8. The similarities of the temperature dependences indicate that the origin of all these peaks is the same. In contrast to the low-temperature phase where the mosaic spread of the crystal is large, the width of the tetragonal peaks and that of the peak at $\xi_t = 0.17$ are comparable to that of the Bragg peaks of the cubic phase. This demonstrates that all these peaks are

caused by dynamic precursor effects, rather than (static) contributions of the low-temperature phase. A further indication for this is that the integral intensity of the central peak at $\xi = 0.33$ is quite low and does not exceed that of the soft phonon. In the previous study¹⁴ this holds only for temperatures above 270 K (50 K higher than T_M), whereas at lower temperatures, where an intermediate phase is supposed, the intensity of the central peak exceeds that of the soft phonon by about a factor of 100.

IV. CONCLUSION

The phonons of Ni₂MnGa were investigated in the ferro- and paramagnetic states. The temperature dependence of the

phonon anomaly of the TA₂ mode at $\xi \approx 0.33$ strongly depends on the magnetic state of the sample, which gives evidence for a magnetic contribution to the Landau free energy. The elastic precursor at the same reduced wave vector coordinate can be assigned to the five-layer modulation of the low-temperature phase. No indication for an intermediate phase, preceding the martensitic transformation, was found.

ACKNOWLEDGMENTS

The susceptibility measurements have been performed by G. Ehlers. We acknowledge support by NATO linkage Grant No. 951422.

-
- ¹ *Proceedings of the International Conference on Martensitic Transformations, ICOMAT-95* [J. Phys. IV **5**, C8 (1995)], and proceedings of previous ICOMAT conferences.
- ² M. Cohen, G. B. Olson, and P. C. Clapp, in *Proceedings of ICOMAT-79*, edited by Department of Material Science and Engineering (MIT, Cambridge, MA, 1979), p. 1.
- ³ L. Delaey, in *Phase Transformations in Materials*, Materials Science and Technology, Vol. 5, edited by P. Haasen (VCH, Weinheim, 1991), p. 339.
- ⁴ S. C. Moss, Mater. Sci. Eng. A **127**, 215 (1990).
- ⁵ P. A. Lindgård and O. G. Mouritsen, Phys. Rev. Lett. **57**, 2458 (1986).
- ⁶ J. A. Krumhansl and R. J. Gooding, Phys. Rev. B **39**, 3047 (1989).
- ⁷ B. Strauss, F. Frey, W. Petry, J. Trampenau, K. Nicolaus, S. M. Shapiro, and J. Bossi, Phys. Rev. B **54**, 6035 (1996).
- ⁸ S. M. Shapiro, B. X. Yang, G. Shirane, Y. Noda, and L. E. Tanner, Phys. Rev. Lett. **62**, 1298 (1989).
- ⁹ S. M. Shapiro, B. X. Yang, Y. Noda, L. E. Tanner, and D. Schryvers, Phys. Rev. B **44**, 9301 (1991).
- ¹⁰ L. E. Tanner, D. Schryvers, and S. M. Shapiro, Mater. Sci. Eng. A **127**, 205 (1990).
- ¹¹ P. J. Webster, K. R. A. Ziebeck, S. L. Town, and M. S. Peak, Philos. Mag. B **49**, 295 (1984).
- ¹² V. V. Martinov and V. V. Kokorin, J. Phys. III **2**, 739 (1992).
- ¹³ V. A. Chernenko, V. V. Kokorin, and I. N. Vitenko, Smart Mater. Struct. **3**, 80 (1994).
- ¹⁴ A. Zheludev, S. M. Shapiro, P. Wochner, A. Schwartz, M. Wall, and L. E. Tanner, Phys. Rev. B **51**, 11 310 (1995).
- ¹⁵ P. Vorderwisch, U. Stuhr, and S. Hautecler (unpublished).
- ¹⁶ V. A. Chernenko, V. V. Kokorin, A. N. Vasil'ev, and Yu. I. Savchenko, Phase Transit. **43**, 187 (1993).
- ¹⁷ A. N. Vasil'ev, V. V. Kokorin, I. Savchenko, and V. A. Chernenko, Sov. Phys. JETP **71**, 803 (1990).
- ¹⁸ J. Worgull, E. Petty, and J. Trivisino, Phys. Rev. B **54**, 15 695 (1996).
- ¹⁹ G. Fritsch, V. V. Kokorin, and A. Kempf, J. Phys.: Condens. Matter **6**, L107 (1994).
- ²⁰ W. Cochran, *The Dynamics of Atoms in Crystals* (Edward Arnold, London, 1973).
- ²¹ R. A. Cowley, in *Structural Phase Transitions*, edited by A. D. Bruce and R. A. Cowley (Taylor & Francis, London, 1981).
- ²² J. A. Krumhansl, Solid State Commun. **84**, 251 (1992).
- ²³ K. Tajima, Y. Endoh, Y. Ishikawa, and W. G. Stirling, Phys. Rev. B **37**, 519 (1976).
- ²⁴ M. Sato, B. H. Grier, S. M. Shapiro, and H. Miyajima, J. Phys. F **12**, 2117 (1982).
- ²⁵ U. Stuhr, P. Vorderwisch, and V. V. Kokorin, Physica B **234-236**, 135 (1997).
- ²⁶ V. V. Martinov, J. Phys. IV **5**, C8-91 (1995).
- ²⁷ *Anharmonic Lattices, Structural Transitions and Melting*, edited by T. Riste (Noordhoff, Leiden, 1974).
- ²⁸ *The Chance to Scatter Neutrons*, edited by A. T. Skjeltorp and O. Steinsvoll (Institute for Energy Technology, Kjeller, and Norwegian Academy of Science and Letters, Oslo, 1997).